Detoxification of Microcystins (Cyanobacterial Hepatotoxins) Using TiO$_2$ Photocatalytic Oxidation

L I N D A   A.   L A W T O N , *,†
P E T E R   K.   J.   R O B E R T S O N ,†
B E N J A M I N   J.   P.   A.   C O R N I S H ,†   A N D
M A R C E L   J A S P A R S ‡

School of Applied Sciences, The Robert Gordon University, Aberdeen, AB25 1HG, U.K., and Department of Chemistry, University of Aberdeen, Old Aberdeen, AB24 3UE, U.K.

TiO$_2$ photocatalysis has been used to destroy microcystin-LR in aqueous solution. The destruction of this toxin was monitored by HPLC, and the disappearance was accompanied by the appearance of seven UV detectable compounds. Spectral analysis revealed that some of these compounds retained spectra similar to the parent compound suggesting that the Adda moiety, thought to be responsible for the characteristic spectrum, remained intact whereas the spectra of some of the other products was more radically altered. Six of the seven observed reaction products did not appear to undergo further degradation during prolonged photocatalysis (100 min). The degree to which microcystin-LR was mineralized by photocatalytic oxidation was determined. Results indicated that less than 10% mineralization occurred. Mass spectral analysis of the photocatalyzed microcystin-LR allowed tentative characterization of the reaction process and products. Reduction in toxicity due to the photocatalytic oxidation was evaluated using an invertebrate bioassay, which demonstrated that the disappearance of microcystin-LR was paralleled by a reduction in toxicity. These findings suggest that photocatalytic destruction of microcystins may be a suitable method for the removal of these potentially hazardous compounds from drinking water.

Introduction

The occurrence of hepatotoxin-producing cyanobacteria is well-documented in freshwaters around the world (*1, 2*), and they are recognized as a potential threat to human health. Risk may be through acute exposure resulting in hepatic injury, which can in extreme cases prove fatal. One such incident occurred recently that resulted in the death of around 50 dialysis patients due to the use of microcystin-contaminated water in their treatment (*3*). Chronic exposure can occur due the presence of microcystins in drinking water and is thought to be a contributing factor in primary liver cancer through the known tumor-promoting activities of these compounds (*4*).

Microcystins are a family of cyclic heptapeptides with the generic structure cyclo(D-Ala-X-D-MeAsp-Z-Adda-D-Glu-Mdha) where Adda is an unusual 20 carbon amino acid, Mdha

* Corresponding author phone: +44 1224 262823; fax: +44 1224 262828; e-mail: l.lawton@rgu.ac.uk.
† The Robert Gordon University.
‡ University of Aberdeen.

is *N*-methyldehydroalanine, and X and Z are variable amino acids (*5*). The structure of microcystin-LR, the subject of this study, is shown in Figure 1. Microcystins are typically produced by planktonic cyanobacteria, which are increasingly found in water bodies at high densities (water blooms) as a result of eutrophication. Many of the water bodies in which microcystin-producing blooms occur are used for drinking water supply, and it is believed that conventional water treatment methods are ineffective in removing these toxins from potable supplies (*6, 7*). Microcystins have been found to be relatively stable across a range of pH and temperature, probably as a result of their cyclic structure. However, they have been found to be degraded in the presence of strongly oxidizing conditions such as high levels of chlorine or ozonation (*7–9*).

In recent years, photocatalytic oxidation using a TiO$_2$ catalyst has received considerable attention. Applications include treatment of wastewaters, removal of noxious organics in potable water, and disinfection (*10–14*). It would appear that this method has a number of advantages over conventional methods, namely, that it does not involve potentially toxic reagents, and in many respects it can be seen as a sustainable treatment method. On illumination of the semiconductor, an electron is promoted from the valence band to the conductance band. For many photocatalytic destruction processes, it has been proposed that hydroxide ions adsorbed to the surface of the catalyst are oxidized to hydroxyl radicals by the photogenerated hole in the valence band. These hydroxyl radicals consequently act as the disinfecting agent in the water. The electron in the conductance band is donated to oxygen generating the superoxide radical anion. The hydroxyl radicals produced by this method are far more oxidizing (2.8 V vs NHE) than many materials that are commonly used for disinfection of water, including ozone (2.07 V vs NHE), hydrogen peroxide (1.78 V vs NHE), hypochlorous acid (1.49 V vs NHE), and chlorine (1.36 V vs NHE) (*12*). Other workers, however, have proposed that the destruction of pollutants may occur by direct valence band oxidation (*15*). Okamoto (*16*) and Anpo (*17*) have proposed that the species formed as a result of the conductance band electron transfer to oxygen (O$_2^{\bullet-}$, HO$_2^{\bullet}$, and H$_2$O$_2$) are also involved in the photooxidation reactions. The role of superoxide and peroxide generated from this species has been discussed in detail by Hoffmann et al. (*13*), Heller et al. (*18*), and Fujishima et al (*19*).

It was recently shown that microcystin-LR was rapidly destroyed by photocatalysis using TiO$_2$, even at extremely high toxin concentrations (*20*); however, little is known about the identity and toxicity of the reaction products. In this study, the products of degradation are assessed including evaluation of the degree to which microcystin-LR is mineralized by this process. Mass spectral analysis is undertaken to tentatively identify the reaction products and possible mechanism of degradation. Toxicity of the breakdown products is assessed by a previously established bioassay for microcystins that uses the brine shrimp *Artemia salina*.

Experimental Section

Chemicals. Microcystin-LR was purified from a naturally occurring bloom of *Microcystis aeruginosa* using the method previously described by Edwards et al. (*21*). Titanium dioxide (Degussa P-25) was used as received. All solutions were prepared in Milli-Q water, and all organic solvents used were analytical grade.

Photocatalysis. Aqueous solutions of microcystin-LR (reaction pH 4 and temperature 306 K) were illuminated in
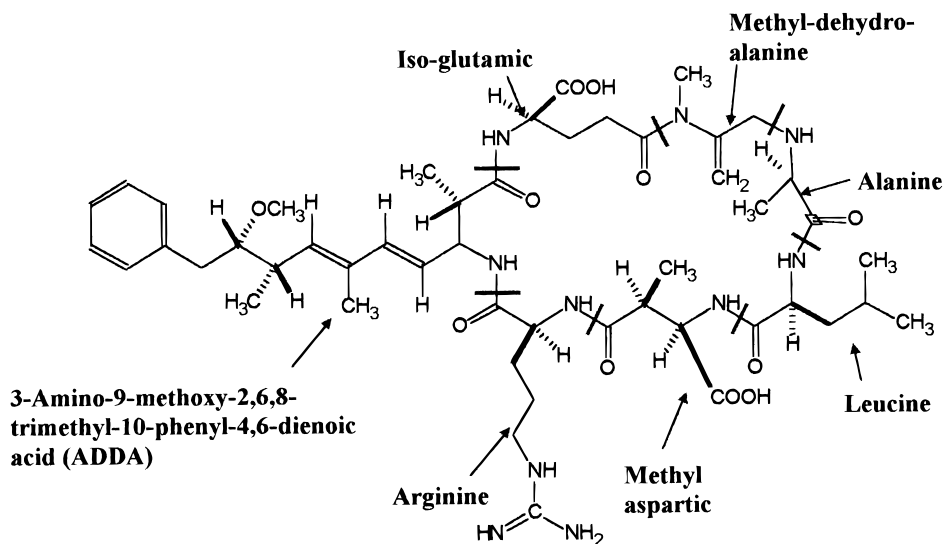
FIGURE 1. Microcystin-LR.

the presence of air and TiO$_2$ catalyst (1% m/v) using a xenon UV lamp (280 W UVASpot 400 lamp, Uvalight Technology Ltd; spectral output 330−450 nm). All reactions were carried out in thick-walled glass universal bottles with constant stirring. Samples were taken at time intervals and centrifuged to remove catalyst prior to quantification by HPLC. The concentration of microcystin-LR (ca. 200 μg mL^{-1}) used in this investigation was considerably higher than might be expected to occur in the natural environment; however, this enabled direct analysis of the toxin and reaction products by HPLC without multistep processing that would be necessary to quantify the much lower levels found in the environment.

Analytical Methods. Analysis of microcystin-LR was performed by HPLC with photodiode array detection as described elsewhere (22) with the following modifications: column, Symmetry C18 250 × 4.6 mm i.d.; detection, Waters 996 high-resolution diode array monitoring between 200 and 300 nm. Spectra of all peaks were compared to those in a microcystin library. Chromatograms were analyzed and integrated at 238 nm. Mass spectrometry was performed using a Finnegan Masslab Navigator, with electrospray ionization. This instrument utilizes a quadrupole mass filter enabling measurement up to 1600 m/z.

Mineralization. The extent of microcystin-LR mineralization due to the photocatalytic process was monitored using a conductivity method similar to those described by Matthews and Byrne (23, 24). A closed system containing the catalyst and microcystin solution was sparged with oxygen instead of air as in the previous experiments. The gas stream from the reaction vessel was bubbled through a Ba(OH)$_2$ conductivity cell. The generation of CO$_2$ results in the production of insoluble BaCO$_3$, reducing the conductivity of the solution in the conductivity cell. The conductivity cell was calibrated by passing predetermined quantities of CO$_2$ through the unit and measuring the conductivity change. This was achieved by injection of Na$_2$CO$_3$ solutions of known concentration into 2 M H$_2$SO$_4$ in a sealed flask. The CO$_2$ generated in the flask was carried over to the conductivity cell by continual purging with CO$_2$-free nitrogen. The resulting change in conductivity was subsequently measured. The calibration plot was prepared by plotting change in conductivity against the quantity of carbon added to the H$_2$SO$_4$.

Toxicity Assessment. Toxicity was determined by brine shrimp bioassay (25) in which 100 mg of *A. salina* eggs (stored at −20 °C until required) was added to 100 mL of brine shrimp media (26) and incubated at 25 °C for 48 h. The newly hatched larvae were separated from unhatched eggs and egg cases,
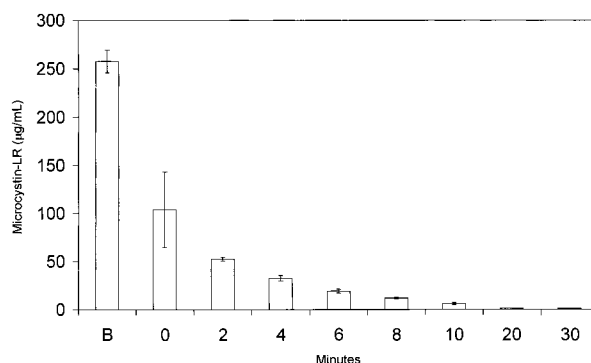

FIGURE 2. Destruction of microcystin-LR by TiO$_2$ photooxidation monitored by HPLC. Bars are equivalent to 1 SD ($n = 2$).

and 100 μL of larvae suspension containing around 30 individuals was placed in each well of a 96-well plate. Microcystin-LR solutions before and after photocatalysis were filtered (0.22 μm) to remove any remaining particles of catalyst. Test solutions were adjusted to the same salt concentration as the media by addition of the appropriate amount of undiluted stock brine shrimp media. A dilution series from 0 to 100 μg mL^{-1} in 10 μg mL^{-1} increments were prepared for each of the exposure times (0, 2, 4, 6, 8, 10, 20, and 30 min) and for the starting solution of microcystin-LR before the addition of catalyst. For each of the dilution series and exposure times, 100 μL of test solution was added to each of four replicate wells containing brine shrimps. Brine shrimps were incubated in the presence of test solutions for 18 h at 25 °C and LC$_{50}$ values for each treatment calculated.

Results and Discussion

Microcystin-LR appeared to be rapidly degraded on exposure to TiO$_2$ and light (Figure 2). This destruction was not observed when microcystin was illuminated in the absence of TiO$_2$. An initial decline in toxin concentration of over 50% was observed on addition of the catalyst, prior to illumination. This was previously observed and referred to as the dark adsorption reaction (20), which is thought to correspond to the adsorption of microcystin-LR onto the surface of the catalyst. Photocatalytic oxidation of microcystin-LR was found to be very rapid, even at the relatively high concentration used in this study, with little toxin detectable by HPLC
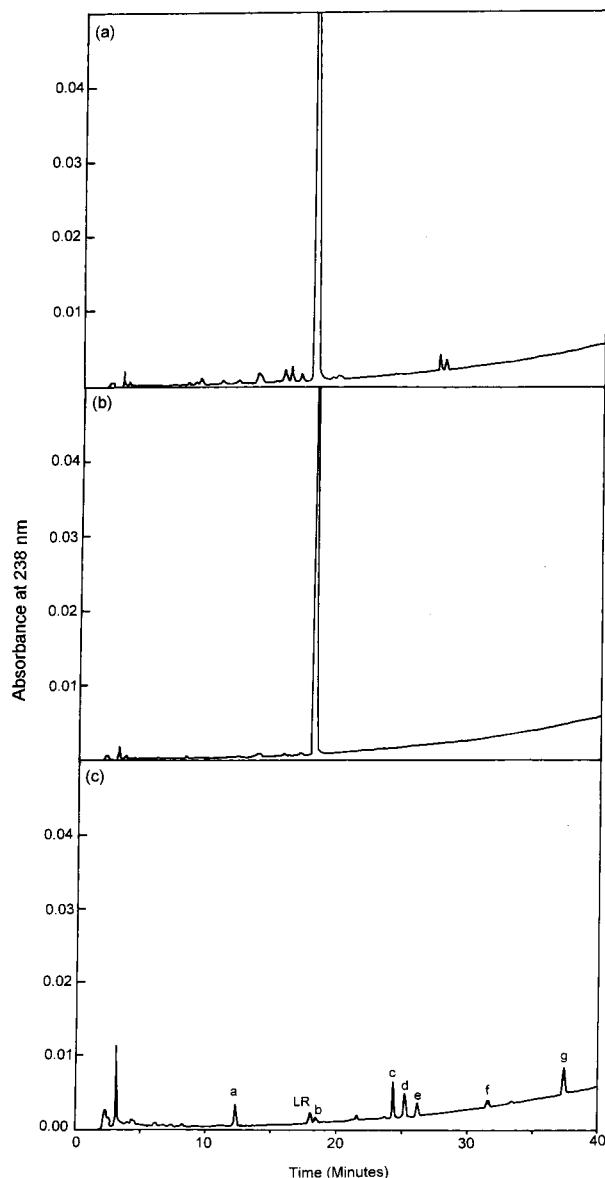
FIGURE 3. HPLC chromatogram of (a) microcystin-LR prior to addition of TiO₂; (b) after addition of TiO₂, not illuminated; and (c) after 10 min photocatalytic oxidation with TiO₂.

after 20 min. Following complete disappearance of microcystin-LR, the catalyst was subjected to solvent extraction to determine if residual toxin was adsorbed to the surface. No residual toxin was detected on the TiO_2 surface.

Analysis of the reaction mixture after photocatalytic treatment revealed a number of UV absorbent products. Of these, seven distinct peaks were observed on the chromatogram that had not been present in the starting material (Figure 3). No novel peaks were observed when microcystin-LR was added to TiO_2 in the absence of UV light or when TiO_2 was added to water alone and illuminated. The absorbance spectrum between 200 and 300 nm of each peak was analyzed and compared to the parent compound. The similarity of each spectrum to that of authentic microcystins was evaluated by use of a spectral library. Closeness of fit is indicated by match angle, where the closer this value is to zero the nearer the spectral match. Four of the peaks (a, b, d, and f) gave no match as determined by a match angle which were found to be >10.000; however, all retained λ_{max} which were less than 10 nm different from the parent compound (Figure 4). Of the remaining three peaks, two were found to have spectra relatively similar to those in the library, with match

angles of 3.196 for peak c and 4.021 for peak g. Peak e gave a match (9.996) that was just below the cutoff, and when studied more closely, its spectrum is very similar to closely eluting peak d. Most of the reaction product peaks (b, d, e, f, and g) appeared rapidly (i.e., in the first 10 min of photocatalytic exposure), which coincides with the rapid decline in detectable microcystin-LR (Figure 4). Furthermore, after their appearance the concentration of these five peaks remained relatively constant throughout the duration of the observed reaction (100 min). However, peak a was seen to increase more gradually until 30 min and then showed a slight decline, although the data were also highly variable, particularly in the later part of the reaction period.

Peak c behaved quite differently from all the other observed reaction products in that, although it appeared rapidly like most of them, it was found to be gradually degraded over the duration of the reaction (Figure 4). Interestingly, this was the reaction product that gave the closest spectral match (3.196) to that of authentic microcystin. It can therefore be speculated that this product is only a slight modification of the parent compound and is itself sensitive to photocatalytic degradation.

To further elucidate the nature of the photocatalytic products of microcystin-LR, the reaction mixture was analyzed by electrospray MS. The breakdown products that might be proposed on the basis of mass spectral data are given in Figure 5. The initial reaction is the dihydroxylation of either of the double bonds of microcystin-LR (Figure 5, structure **1**), witnessed by the increase from 995.7 m/z [M + H]⁺ to 1029.7 m/z [(M + 2OH) + H]⁺ (Figure 5, structures **2** and **3**). At the same time 835.5 m/z [M + H]⁺ becomes prominent, and this is consistent with cleavage occurring at Adda CH= CMe (Figure 5, structure **4**). Also at this time a smaller peak at 817.5 m/z appears; this is consistent with the cleavage occurring at Adda CH=CH [M + Na]⁺ (Figure 5, structure **5**). After a further 10 min, the peak at 835.5 m/z disappears and a peak at 817.5 m/z becomes dominant. The proposed mechanism is then that dihydroxylation occurs at either of the Adda double bonds, followed by cleavage. The reason that the 835.5 m/z disappears altogether can be due to the fact that a further cleavage step may occur at Adda CH=CH via structure **6** in Figure 5 giving rise to structure **5**. This is a very stable product, as is witnessed by the fact that it is present up to 100 min. Future studies are aimed at delineating the exact nature of the mechanism by high-resolution MS and isolating the products using HPLC and identifying them using a combination of MS and NMR. Since hydroxylated products were detected, it would appear that the photocatalytic destruction process is initiated by hydroxyl radical attack on the microcystin. This premise is supported by the observation of a primary kinetic isotope effect of 3 for the process that has been reported previously (27). It is however possible that the toxin undergoes a direct oxidation at the valence band of TiO_2. The radical cation formed from this process could then react with water forming the same hydroxylated products.

The mass spectral fragmentation data is supported by the UV spectra acquired during the HPLC runs. The calculated value of λ_{max} for microcystin Adda is 240 nm (including solvent correction), which is identical to that of the observed value (28). The rapid increase in peak c in the HPLC trace followed by its rapid decrease is similar to the behavior of 835 m/z in the MS. The MS suggested that this was structure **4** in Figure 5, and the calculated UV λ_{max} for structure **4** is 235 ± 5 nm, which is consistent with the observed value of 239 nm. Structures **2**, **3**, **5**, and **6** in Figure 5 are not expected to have observable UV spectra since the UV chromaphore has been removed as a result of the photocatalytic process.

It is clear from the preceding findings that microcystin-LR has not been completely mineralized in contrast with
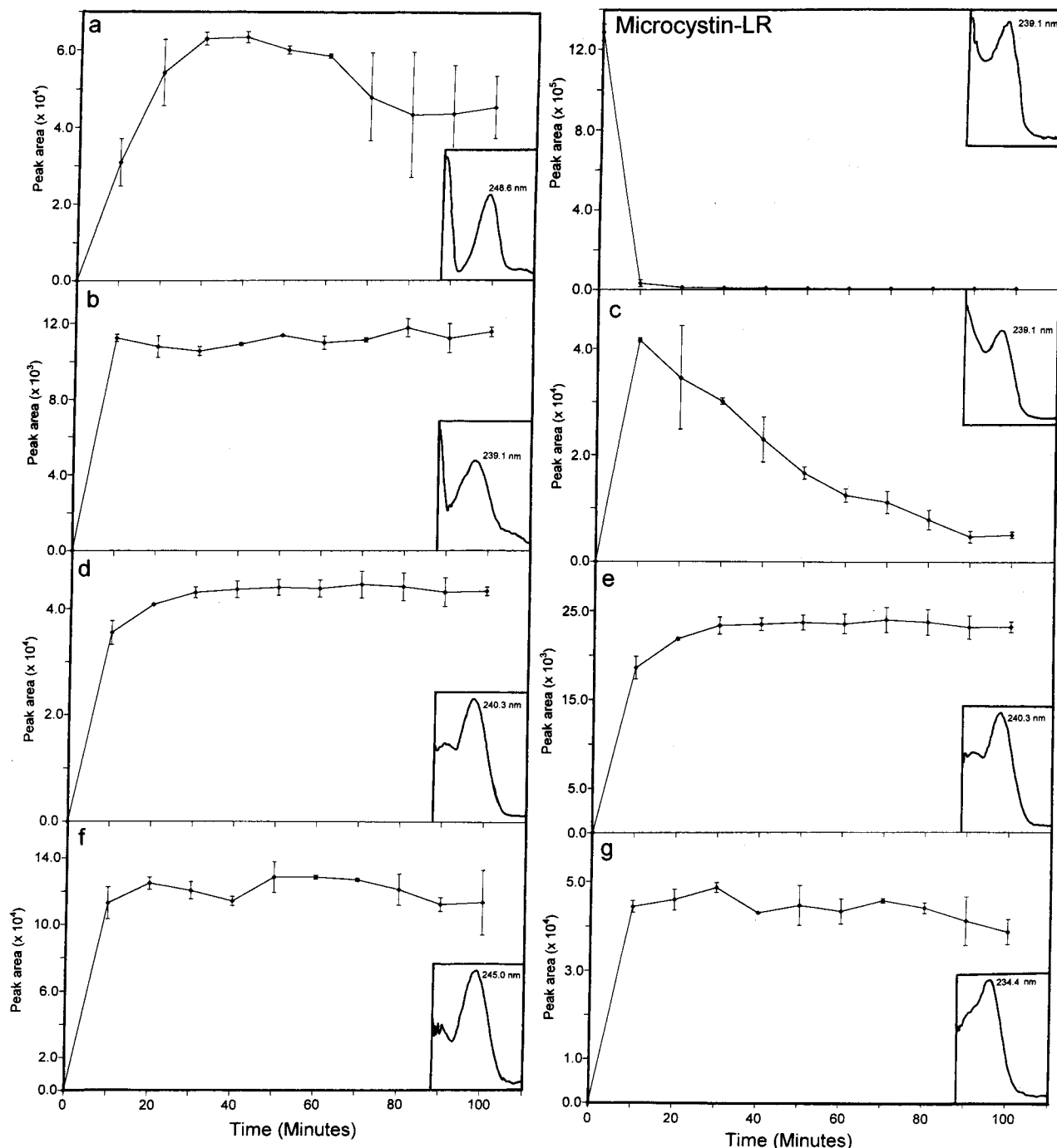
FIGURE 4. Presence of microcystin-LR and seven reaction products detected by HPLC during prolonged TiO₂ photooxidation, with inserts showing the absorbance spectrum (200−300 nm) of each peak and λ_{max}. Bars represent 1 SD (n=2).

other simpler organic compounds that demonstrated total mineralization. The complete mineralization of a range of halogenated hydrocarbons has been reported by a number of researchers (16, 29−31) who investigated the photocatalytic mineralization of dichloromethane, chloroform, carbon tetrachloride, trichloroethylene, phenol, and chlorobenzene. The degree to which microcystin-LR was mineralized was determined using a simple conductivity method, and this indicated that 6.4% of the total compound has been mineralized confirming that many of the reaction products are stable and do not under go complete degradation.

Since it was shown that the toxin is not completely degraded, it is important to confirm that the photocatalytic breakdown products were nontoxic. To assess this, a simple invertebrate bioassay was carried out. It was found that the toxicity data corresponded well with the HPLC findings (Table 1). Reduction in toxicity mirrored the reduction in the concentration of microcystin-LR that was seen to occur over the first 10 min of the photocatalytic treatment. As with the HPLC analysis, toxicity dropped on the addition of the TiO₂ catalyst, which was explained by the dark reaction (Table 1). On illumination, toxicity dropped further, and all samples tested after 8 min were of low toxicity; therefore, an LC_{50} value could not be detected. These findings suggest that TiO₂ photocatalysis does in fact eliminate the toxicity associated with microcystin-LR and indicate that although the toxin is not completely mineralized it is rendered safe. It will, however, be important to carry out further studies to fully characterize the observed reaction products and where
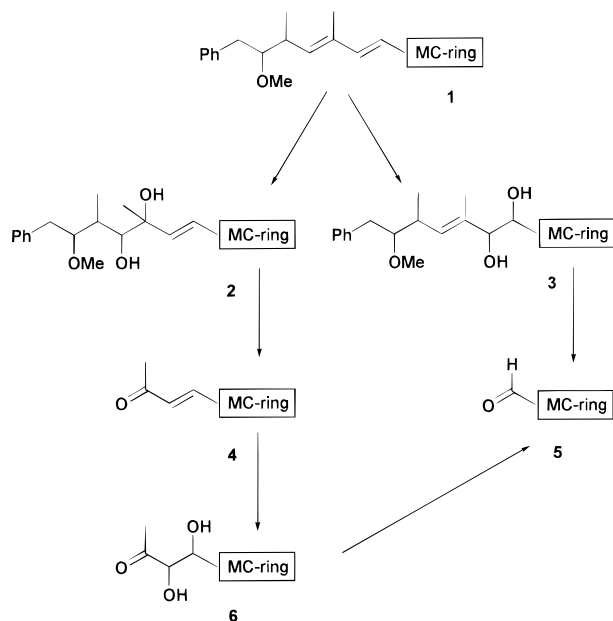
FIGURE 5. Scheme of proposed microcystin-LR breakdown products following TiO₂ photocatalysis based on mass spectral data.

TABLE 1. Effect of Photocatalytic Oxidation on the Toxicity of Microcystin-LR, Determined by Brine Shrimp Bioassay

exposure time (min)	LC_{50} (μg/mL)	exposure time (min)	LC_{50} (μg/mL)
starting solution[a]	2.0	6	41.3
		8	>50.0
0	10.8	10	>50.0
2	17.3	20	>50.0
4	27.5	30	>50.0

[a] Microcystin-LR solution prior to the addition of TiO₂.

possible assess their toxicity individually. Furthermore, analysis of the protein phosphatase inhibition activity of the reaction products will be vital to confirm that water treated in this way will be safe to drink, showing that the tumor-promoting potential that results from protein phosphatase inhibition has been removed.

It is clear that TiO₂ photocatalysis has great potential as a reliable method for the detoxification of water contaminated with cyanobacteria hepatotoxins. Although the work carried out here has been performed using only one microcystin congener and it is known that at least 60 variants have been described (32), it is believed that due to their structural similarity that this method will be effective for all variants. However, it will be wise to assess at least some of the other commonly occurring microcystins to confirm the efficacy of this method for these toxicants.

In conclusion, TiO₂ catalyzed photodegradation effectively and rapidly degraded microcystin-LR and in doing so removed the toxicity associated with this compound. Further work must now be carried out to optimize the process and evaluate its performance at both environmentally relevant concentrations and in a range of water types.

Literature Cited

(1) Carmichael, W. W. In *Manual on Harmful Marine Microalgae*; Hallegraeff, G. M., Anderson, D. M., Cembella, A. D., Eds.; United Nations Educational, Scientific and Cultural Organization: Paris, 1995.
(2) Sivonen, K. *Phycologia* **1996**, *35*, 12−24.
(3) Dunn, J. *Brit. Med. J.* **1996**, *312*, 1183−1184.
(4) Yu, S.-Z. In *Toxic Cyanobacteria: Current Status of Research and Management*; Steffensen, D. A., Nicholson, B. C., Eds.; Australian Centre for Water Quality Research: Salisbury, Australia, 1994.
(5) Botes, D. P.; Wessels, P.; L. Kruger, H.; Runnegar, M. T. C.; Santikarn, S.; Smith, R. J.; Barna, J. C. J.; Williams, D. H. J. *Chem. Soc. Perkins Trans.* **1985**, *1*, 2747−2748.
(6) Lahti, K.; Hiisvirta, L. *Water Supply* **1989**, *7*, 149−154.
(7) Keijola, A. M.; Himberg, K.; Esala, A. L.; Sivonen, K.; Hiisvirta, L. *Toxicol. Assess.* **1988**, *3*, 643−656.
(8) Nicholson, B. C.; Rositano, J.; Burch, M. D. *Water Res.* **1994**, *28*, 1297−1303.
(9) Tsuji, K.; Watanuki, T.; Kondo, F.; Watanabe, M. F.; Nakazawa, H.; Suzuki, M.; Uchida, H.; Harada, K.-I. *Toxicon* **1997**, *35*, 1033−1041.
(10) Jakob, L.; Oliveros, E.; Legrini, O.; Braun, A. M. In *Photocatalytic Purification and Treatment of Water and Air*; Ollis, D. F., Al-Ekabi, H., Eds.; Elsevier Science: Amsterdam, 1993.
(11) Schmelling, D. C.; Gray, K. A.; Kamat, P. V. *Water Res.* **1997**, *31*, 1439−1447.
(12) Robertson, P. K. J. *J. Cleaner Prod.* **1996**, *4*, 203−212.
(13) Hoffmann, M. R.; Martin, S. T.; Choi, W.; Bahnemann, D. W. *Chem. Rev.* **1995**, *95*, 69−96.
(14) Mills, A.; Le Hunte, S. *J. Photochem. Photobiol. A* **1997**, *108*, 1−35.
(15) Draper, R. B.; Fox, M. A. *Langmuir* **1990**, *6*, 1396−1402.
(16) Okamoto, K.; Yamamoto, Y.; Tanaka, H.; Tanaka, M.; Itaya, A. *Bull. Chem. Soc. Jpn.* **1985**, *58*, 2015−2022.
(17) Anpo, M.; Chiba, K.; Tominari, M.; Coluccia, S.; Che, M.; Fox, M. A. *Bull. Chem. Soc. Jpn.* **1991**, *64*, 543−551.
(18) Schwitzgebel, J.; Ekerdt, J. G.; Gerischer, H.; Heller, A. *J. Phys. Chem.* **1995**, *99*, 5633−5638.
(19) Ikeda, K.; Hashimoto, K.; Fujishima, A. *J. Electroanal. Chem.* **1997**, *437*, 241−244.
(20) Robertson, P. K. J.; Lawton, L. A.; Münch, B.; Rouzade, J. *J. Chem. Soc. Commun.* **1997**, *4*, 393−394.
(21) Edwards, C.; Lawton, L. A.; Coyle, S. M.; Ross, P. *J. Chromatogr. A* **1996**, *734*, 163−173.
(22) Lawton, L. A.; Edwards, C.; Codd, G. A. *Analyst* **1994**, *119*, 1525−1530.
(23) Matthews, R. W.; Abdullah, M.; Low, G. K.-C. *Anal. Chim. Acta* **1990**, *233*, 171−179.
(24) Byrne, J. A. Ph.D. Thesis, University of Ulster, Belfast, 1997.
(25) Campbell, D. L.; Lawton, L. A.; Beattie, K. A.; Codd, G. A. *Environ. Toxicol. Water Qual.* **1994**, *9*, 71−77.
(26) Harwig, J.; Scott, P. M. *Appl. Microbiol.* **1971**, *21*, 1011−1016.
(27) Robertson, P. K. J.; Lawton, L. A.; Cornish, B. J. P. A.; Jaspars, M. *J. Photochem. Photobiol. A* **1998**, *116*, 215−219.
(28) Crews, P.; Rodriguez, J.; Jaspars, M. In *Organic Structure Analysis*; Oxford University Press: New York, 1998.
(29) Pruden, L.; Ollis, D. *J. Catal.* **1983**, *82*, 404−417.
(30) Matthews, R. W.; Ollis, D. F. *J. Catal.* **1986**, *97*, 565−569.
(31) Hsiao, C.-Y.; Lee. C.-Y.; Ollis, D. F. *J. Catal.* **1983**, *82*, 418−423.
(32) Carmichael, W. W. *Adv. Bot. Res.* **1997**, *27*, 212−256.